Heliyon 10 (2024) e36063

Contents lists available at ScienceDirect

Heliyon

journal homepage: www.cell.com/heliyon

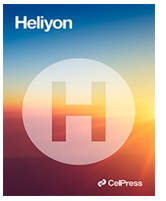

Research article

Forskolin improves experimental autoimmune encephalomyelitis in mice probably by inhibiting the calcium and the IL-17-STEAP4 signaling pathway

Qinyao Yu [b], Mengqing Li [a], Umer Anayyat [a], Cai Zhou [a], Shenglan Nie [a], Hua Yang [a], Fengyi Chen [b], Shuling Xu [b], Yunpeng Wei [a,**], Xiaomei Wang [a,c,*]

[a] School of Basic Medical Sciences, Shenzhen University, Shenzhen, Guangdong, 518061, China
[b] School of Pharmacy, Shenzhen University, Shenzhen, Guangdong, 518061, China
[c] International Cancer Center, Shenzhen University Health Sciences Center, Shenzhen, Guangdong, 518061, China

ARTICLE INFO

Keywords:
Forskolin
Multiple sclerosis
STEAP4
Interleukin 17
The calcium signaling pathway

ABSTRACT

Multiple sclerosis (MS) is a chronic autoimmune disease in the central nervous system. Forskolin (FSK) is a plant-derived diterpene with excellent immunomodulatory properties and has not been systematically reported for treating MS. This study investigated the therapeutic effects of FSK on cellular and animal MS models and preliminarily explored related mechanisms. The results showed that FSK suppressed the inflammatory response, reduced the expression of STEAP4, and relieved iron deposition in BV-2 cells pretreated by LPS at the cellular level. Meanwhile, at the animal level, FSK treatment halted the progression of experimental autoimmune encephalomyelitis (EAE), alleviated the damage at the lesion sites, reduced the concentration of proinflammatory factors in peripheral blood, and inhibited the immune response of peripheral immune organs in EAE mice. Besides, FSK treatment decreased the expression of STEAP4 in the spinal cord and effectively restored the iron balance in the brain, spinal cord, and serum of EAE mice. Further investigation showed that FSK can reduce IL-17 expression, prevent the differentiation of TH17 cells, and inhibit the calcium signaling pathway. Thus, these results demonstrate that FSK may have the potential to treat MS clinically.

1. Introduction

Multiple sclerosis (MS) is a chronic autoimmune disease of the central nervous system (CNS) characterized by inflammatory demyelinating lesions, cellular and humoral immune disorders, white matter damage [1], and a remarkable imbalance of metal ions, including iron and copper [2]. Epidemiological surveys have shown that the overall incidence of MS is 5.7/10,000, with a high incidence between the ages of 15~44, and a significantly higher incidence in women than in men was observed [3].

Experimental autoimmune encephalomyelitis (EAE) in mice, a widely used animal MS model, can assist the study of synaptic changes during autoimmune attacks and corroborate findings in the human MS brain [4]. EAE is a predominantly sensitized $CD4^+$ T cell-mediated disease characterized by the presence of mononuclear leukocytes infiltration and myelin loss around small blood vessels

* Corresponding author. School of Basic Medical Sciences, Shenzhen University, Shenzhen, Guangdong, 518061, China.
** Corresponding author.
E-mail addresses: wyp@szu.edu.cn (Y. Wei), xmwang@szu.edu.cn (X. Wang).

https://doi.org/10.1016/j.heliyon.2024.e36063
Received 28 March 2024; Received in revised form 18 July 2024; Accepted 8 August 2024
Available online 10 August 2024

in the CNS. It can be induced by the active immunization of animals with myelin antigens or by the relay transfer of myelin antigen-specific T cells. In the active EAE model, auto-reactive myelin-specific effector T cells are formed in peripheral lymph nodes and migrate into the CNS to trigger autoimmune responses, leading to MS-like symptoms [5].

Interleukin 17 (IL-17) has recently been reported to be one of the most important players in MS and other autoimmune diseases [6]. In recent years, the importance of IL-17 in human MS and EAE mice has received much more attention [7]. $CD4^+$, $CD8^+$ T cells, and B cells are involved in the development of the disease. Th1 cells were considered the main inflammatory mediator cells leading to neurological damage until the effects of IL-17 were identified [8]. IL-17 is a group of T cell-derived cytokines including six family members (IL-17A, B, C, D, E, F), and there are five known receptors (IL-17RA, IL-17RB, IL-17C, IL-17RD, and SEF). IL-17 is mainly secreted by $CD4^+$ Th17 cells, which promote the activation of T cells and induce the synthesis and secretion of various cytokines such as IL-6, IL-8, granulocyte-macrophage stimulating factor (GM-CSF), and prostaglandin. IL-17 plays a crucial role in the development of MS and EAE. Due to the expression of IL-17RA in astrocytes of human and mice, IL-17 can induce astrocytes to produce cytokines and chemokines including IL-6, TNFα, CCL2, CCL3, CCL20, CXCL1, CXCL2, CXCL9, CXCL10 and CXCL11 [9]. IL-17 also activates the IL-6R signaling pathway in astrocytes, leading to massive production of CCL20, thus promoting infiltration of CCR6+ Th17 cells at the sites of inflammation [10]. In addition, IL-17 can activate microglial cells to secrete pro-inflammatory factors, which are found in the tissues at sites of demyelinating inflammation in MS patients [11]. IL-17-mediated infiltration of lymphocytes and the release of large amounts of inflammatory mediators are the main causes of nerve fiber demyelination and neurodegeneration [10] (Fig. 1). Thus, the monitoring of Th17 cell/IL-17 levels can be an important predictor of relapse after antibody therapy in MS patients [12]. Besides, in a large-scale phase II clinical trial of IL-17-neutralizing antibodies named Secukinumab for MS treatment, the results showed a 60 % reduction in new MRI lesions and a trend toward lower annual recurrence rate compared with placebo [13]. These findings underscore the potential of IL-17 as a therapeutic target for MS.

It was discovered that iron and copper levels significantly increased in the brain and lesions in the early stages of MS [2,14], and the oxidative stress induced by them may be a common mechanism in the initiation and development of MS and other neurological diseases like AD. Besides, colon cancer tissues overexpressed STEAP4 exhibit enhanced inflammatory response and increased copper uptake [15], and there is also a significant increase in Cu levels in serum and cerebrospinal fluid in MS patients (Fig. 2 [14]), suggesting possible involvement of STEAP4 in MS. In addition, a recent study has demonstrated that IL-17 can increase intracellular Cu levels and induce high expression of STEAP4, which in turn maintains IL-17-mediated NF-κB activity and inhibits the activity of Caspase-3 induced by X-linked inhibitor of apoptosis (XIAP) activation, thus inhibiting the inflammation-induced apoptotic process [16].

Forskolin (FSK) (7beta-acetoxy- 8,13 -epoxy-1a, 6 beta, 9a-trihydroxy-labd-14-en-11-one), a diterpene extracted from *Coleus barbatus* and approved as an anti-inflammatory agent by the DCGI in India in 2006, is a lipid-soluble compound that can penetrate cell membranes and activate adenylate cyclase. Despite a variety of pharmaceutical properties including lowering blood and intraocular pressure, inhibiting platelet aggregation, calming asthma, losing weight, and inhibiting tumors [17], FSK is known for its excellent immunomodulatory properties. In HIV-1 infection, IL-17A and cytokines such as IL-2 and IL-6 were elevated at different stages of infection, while FSK can significantly reduce the level of these inflammatory factors and slow down the progression of HIV infection [18]. Meanwhile, FSK can also downregulate the transcription and expression of TNF-α and IL-6 in mouse macrophages, human macrophages, and dendritic cells, as well as inhibit the inflammatory response in rBmpA-induced arthritis models of mice [19]. Besides, it has also been proven that FSK can inhibit lipopolysaccharide (LPS)-induced inflammatory responses in mononuclear leukocytes [20].

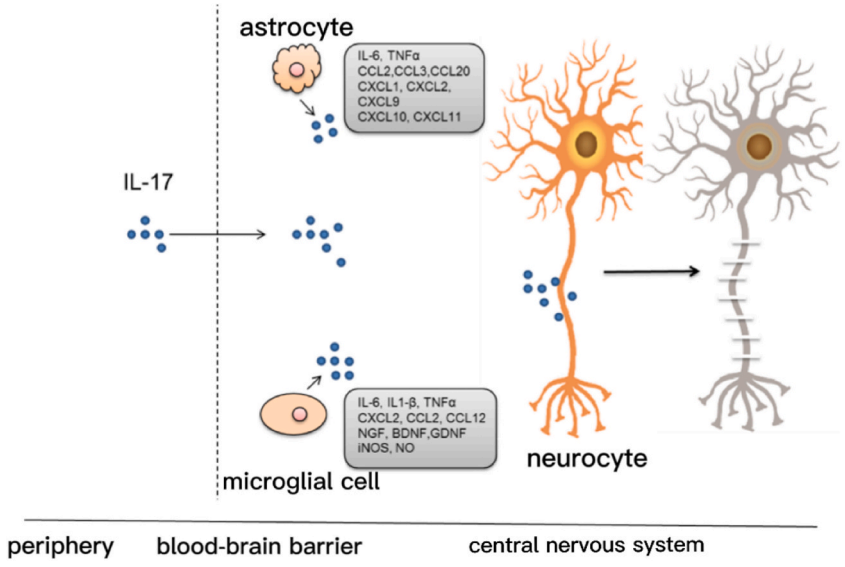

Fig. 1. IL-17 mediates demyelination and inflammatory infiltration of the central nervous system in MS.

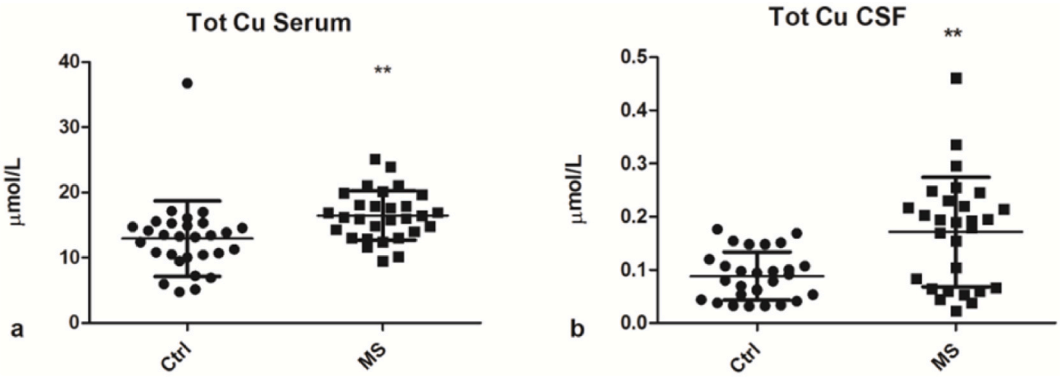

Fig. 2. Changes in Cu levels in serum and cerebrospinal fluid of MS patients [14].

In conclusion, it has been confirmed that FSK indeed has excellent immunomodulatory effects, and MS is a chronic autoimmune disease. However, no systematic study about the therapeutic effects of FSK on MS has been published. Thus, this study investigated the therapeutic effect of FSK on MS models and related mechanisms. We hope our work can provide valuable exploration for the research and screening of therapeutic drugs for MS treatment.

2. Materials and methods

2.1. Mice grouping and treatment

21 C57 female mice (6–8 weeks) were purchased from Guangzhou Yancheng Biotechnology Co. After one week of adaptive feeding in the Animal Center of Shenzhen University, they were randomly divided into three groups ($n = 7$ in each group): the control group (Sham group), the modeling group (EAE group) and the FSK treatment group (EAE-FSK group). All experimental mice were housed in plastic cages in a temperature-controlled room (room temperature 23 ± 1 °C, humidity 55 ± 5 %) with a 12-h light/12-h dark cycle and allowed to access food and water freely.

To prepare EAE model of mice, each mouse in the EAE group and the EAE-FSK group was injected subcutaneously with 300 μL (200 μg) of myelin oligodendrocyte glycoprotein (MOG, Kangbei, China, TQ33371-50) solution (MOG was mixed with Freund's adjuvant (Sigma, USA, F5881) containing 4 mg/mL Mycobacterium tuberculosis equivalently) at 3–4 points on the neck and the sides of the spine on the day of sensitization. Then, on the day of inoculation and 48h later, each of these mice was given an intraperitoneal injection of Pertussis toxin (Jena Bioscience, China, PR-BA120P–S) with a dose of 500 ng. Mice in the control group were injected with the same volume of normal saline. In addition, FSK (purchased from Xi'an Tian Feng Biological Technology Co.) was dissolved in a 5 % ethanol solution and administered by gavage with a dose of 2 mg/kg in the FSK treatment group. Finally, the neurofunctional behavioral scores were used to assess the progression of EAE (see Table 1).

The animal experiment protocols were reviewed and approved by the Animal Ethics Committee of Shenzhen University (Ethical Approval Number: IACUC-202300190), and each procedure was designed to minimize animal suffering and limit the number of animals used.

2.2. Locomotor behavioral test

On the 18th day after immunization, mice were placed individually in Pheno Typer 3000 cages (Noduls, Netherlands) and their movement trajectories were recorded for 30 min (20:00–20:30) after the mice had become familiar with their environment. The trajectories were then mapped using the Ethovision XT V14 processing system (Noduls, Netherlands), their total distance traveled, and the average speed of movement were also calculated.

Table 1
Neurofunctional behavioral scores of EAE model of mice.

Classification	Symptoms
0	Asymptomatic
1	Tail weakness
2	Caudal weakness and incomplete hind limb paralysis
3	Both hind limbs are paralyzed
4	Both hind limbs and either forelimb are paralyzed and cannot be reduced after passive turning
5	On the verge of death

2.3. Luxol Fast Blue Myelin Staining

After the locomotor behavioral test, the mice were sacrificed by cervical dislocation, and the enlarged spinal cord of the lumbar spine was separated. The fresh spinal cord was then fixed in 8 % formalin solution to prepare 6 μm paraffin sections. Luxol Fast Blue Myelin Staining was conducted using a Luxol Fast Blue (LFB) myelin staining kit (Solarbio, China, G3245). Briefly, paraffin sections were dewaxed in 95 % ethanol, followed by the treatment of solid blue staining solution at room temperature for 20 h. The excess staining solution was washed with 95 % ethanol, then washed with distilled water and separated with a solid blue differentiation solution for 15 s. After that, the sections were immersed in 70 % ethanol for 30 s to clear gray matter, then rinsed with distilled water, redyed, washed again, dehydrated, transparentized in xylene, and sealed neutral resin. Finally, the sections were observed under an optical microscope (OLYMPUS, Japan).

2.4. Flow cytometry (FC)

Fresh spleens and lymph nodes were isolated separately in a lymphatic fluid using a cell strainer (Acrodisc®, US). Then,1000 μL of spleen cell suspension was added into RPMI1640 medium and centrifuged at 800 g for 30 min at room temperature. Lymphocyte layers were incubated with FITC anti-CD4 (BD Biosciences, USA, 561833) and PE anti-IL-17A (BD Biosciences, USA, 561020) for 30 min on ice away from light. Data were obtained on a flow cytometer (BD, USA).

2.5. Cell culture

BV-2 cells (Pricella, China, CL-0493A) were cultured in DMEM high glucose medium (Gibco, USA, 11965092) supplemented with 10 % fetal bovine serum, 100 μg/mL penicillin, and 100 μg/mL streptomycin. The cells were then incubated in a cell incubator (ThermoFisher, USA) with 5 % CO_2 at 37 °C.

2.6. Cells grouping and treatment

BV-2 cells were divided into three groups: the Sham group, the LPS group, and the LPS + FSK group.

Sham group: BV-2 cells were cultured in a normal medium for 24 h. Then the cells were treated in a normal medium containing 0.1 % DMSO for 24 h. After removing the medium containing 0.1 % DMSO, the cells were cultured in the same normal medium containing 0.1 % DMSO for 48 h;

LPS group: BV-2 cells were cultured in a normal medium for 24 h. Then, cells were treated with 1 μg/mL LPS for 24 h. After removing the medium containing LPS, the cells were cultured in a normal medium containing 0.1 % DMSO for 48 h;

LPS + FSK group: BV-2 cells were cultured in a normal medium for 24 h. Then, cells were treated with 1 μg/mL LPS for 24 h. After removing the medium containing LPS, the cells were treated in a normal medium containing 6.25 μM FSK for 48 h.

2.7. CCK-8 assay of cell viability

According to the instructions of the kit (MedChemExpress, US, 47910-79-2), 100 μL cells (2000 cells/100 μL) were seeded into each hole of the 96-well plate, and after culturing for 24h, the corresponding treatments (IC_{50} determination and different treatments of each group in 2.6) were carried out. Then, each well was added with 10 μL CCK8 solution, and all the cells were incubated in the incubator for 1h, and the 450 nm OD value of each well was detected using a microplate reader (BioTek, US).

2.8. Cell transfection

BV-2 cells were inoculated into 6-well plates (10^5 cells per well) and cultured for 24 h. Then, the original medium was discarded, the cells were washed with PBS three times, and a new medium containing Polybrene (Beyotime, China, C0351) was added. Then, the *STEAP4*-carrying virus (pSLenti–SFH–EGFP-P2A-Puro-CMV-Steap4-3xFLAG-WPRE, OBiO Technology (Shanghai) Corp., Ltd., China) was added to cells in gradients (5 μL, 10 μL, 50 μL on different pore plates). After continuing the culture for 12 h, the liquid was changed and washed with PBS three times. The successfully transfected cells fluoresced green under a fluorescence microscope. Puromycin (10 mg/mL, 50 μL), after which puromycin (10 mg/mL, 50 μL) was added to kill the non-transfected cells. Finally, BV-2 cells with *STEAP4* overexpression could be obtained by continuous culture of the surviving cells for 24 h.

2.9. Elisa

The levels of IL-6, IL-17A, and IFN-γ in serum and cell supernatant were detected by corresponding ELISA kits (Thermo, US, 88-7064-88) according to the instructions.

2.10. Total Fe content assay

The total Fe content of BV-2 cells, serum, and brain tissue was measured using Elabscience® Total Iron Ion Colorimetric Test Kit (Elabscience®, Canada, E-BC-K772-M) following the instructions. The final detection was performed at 590 nm using a microplate

reader (Tecan, Germany).

2.11. Quantitative real-time PCR

Total RNA was extracted from BV-2 cells, spleen, and brain using Trizol (Takara, Japan, 15596026), and reverse-transcribed to cDNA using Hifair® II 1st Strand cDNA Synthesis Kit (YESEN, China, 11141ES10). Then, PCR of targeted genes was performed using Hieff UNICON® Universal Blue qPCR and SYBR Green Master Mix (YESEN, China) (30 s at 95 °C, 40 cycles of 10 s at 95 °C and 30 s at 60 °C). mRNA of β-actin served as the internal reference. All the primers are shown below (Table 2).

2.12. Western blot

Spinal cord tissue and brain tissue were homogenized in RIPA-containing protease and phosphatase inhibitors (Beyotime, China, P0013B). The lysate was further ultrasonically homogenized and then centrifuged at 5000 rpm at 4 °C for 10 min. After quantifying the protein concentration using the BCA protein assay kit (Thermo Fisher Scientific, Waltham, MA, USA, 23250), the sample was denatured in a metal bath at 95 °C for 10 min. The proteins were then separated with a 7.5–15 % gel and transferred to the PVDF membrane. The PVDF membrane was blocked with 5 % skim milk at room temperature for an hour. The membranes were then incubated at 4 °C overnight with specific antibodies (anti-IL-6, anti-IL-17A, anti–NF–KILB, anti-P-JNK, anti-JNK, anti-NFATC1, anti-STAT3, anti-STEAP4) (SAB, USA). After TBST washing 3 times, the membranes were incubated with the corresponding secondary antibody at room temperature for 1 h. Finally, the protein bands were visualized using the ECL blotting kit (MeilunBio®, China, MA0186) and gel imaging system (Tanon-5220, Shanghai, China), and analyzed using Image J software.

2.13. Statistical analysis

Data were performed as means with standard errors (mean ± SEM) unless otherwise specified and analyzed by the One-way ANOVA test and Dunnett's *t*-test. $P < 0.05$ was considered statistically different.

3. Result

3.1. FSK blocked the inflammatory process caused by LPS and decreased STEAP4 expression in BV-2 cells

According to the CCK-8 assay results of cell viability, the IC_{50} of FSK on BV-2 cells was calculated as 984.93 μM by GraphPad Prism 9.0 (Fig. 3A). In addition, the results of the CCK-8 assay showed that the combination of different concentrations of FSK and LPS did not affect cell viability (Fig. 3B). Elisa assay confirmed 6.25 μM FSK as the subsequent drug treatment concentration, for 6.25 μM FSK induced the lowest level of IL-6 in the supernatant (Fig. 3C). Then, the expression of *CCL-2*, *CCL-3*, *IL-6*, *CXCL-2*, and *CXCL-10* in the cells was detected by qPCR. The results showed that the expression levels of these factors significantly increased in the LPS group compared to the sham group, while they remarkably decreased after 48 h of treatment with FSK compared to the LPS group. In addition, compared with the sham group, the expression levels of these cytokines and chemokines were not significantly different (Fig. 3D). Meanwhile, high-purity BV-2 $STEAP4^+$ cells were successfully constructed, and 6.25 μM FSK treatment alone didn't affect the cell viability (Fig. 3E). It was discovered that the concentration of IL-6 in BV-2 $STEAP4^+$ cells was significantly higher than that in normal BV-2 cells supernatant. The Elisa assay showed a significant decrease in IL-6 in the supernatant of BV-2 $STEAP4^+$ cells after the drug treatment (Fig. 3F). Besides, the qPCR assay showed that *STEAP4* expression significantly decreased after FSK treatment (Fig. 3G) (the expression of *STEAP4* in normal BV-2 cells could not be detected because of its extremely low expression). Finally, the concentration of total iron ions in BV-2 $STEAP4^+$ cells was significantly higher than that in normal BV-2 cells supernatant. However, the content of total iron ions in the supernatant of BV-2 $STEAP4^+$ cells also significantly decreased after FSK treatment (Fig. 3H).

Table 2
The sequence of the forward primer and reverse primer of targeted genes.

	Forward primer	Reverse primer
β-actin	GAGACCTCAACACCCCAG	CATCACAATGCCTGTGGTAC
IL-6	GCCACTCACCTCTTCAGAACGA	CTGGCTTGTTCCTCACTACTCT
STEAP4	GCGC CICTCCCTCAGTTATG	GGTCTTCTGGGGGTTTCGAC
IL-17A	TGTCTCTGATGCTGTTGCT	GTTGACCTTCACATTCTGG
CXCL-10	TGATTTGCTGCCTTATCTTTCTGA	CAGCCTCTGTGTGGTCCATCCTTG
CXCL-9	TGCACGATGCTCCTGCA	AGGTCTTTGAGGGATTTGTAGTGG
CCL-2	CCCAATGAGTAGGCTGGAGA	AAGGCATCACAGTCCGAGTC
CCL-3	CAATTCATCGTTGACTATT	CAGTGATGTATTCTTGGA
CXCL-1	CTTGCCTTGACCCTGAAGCTC	AGCAGTCTGCTTCTTTCTCCGT
CXCL-2	CCCCCTGGTTCAGAAAATCA	GCTCCTCCTTTCCAGGTCAGT
TGF-β	AGGACCTGGGTTGGAAGTGG	AGTTGGCATGGTAGCCCTTG
IFN-γ	AGCAACAACATAAGCGTCATT	CCTCAAACTTGGCAATACTCA

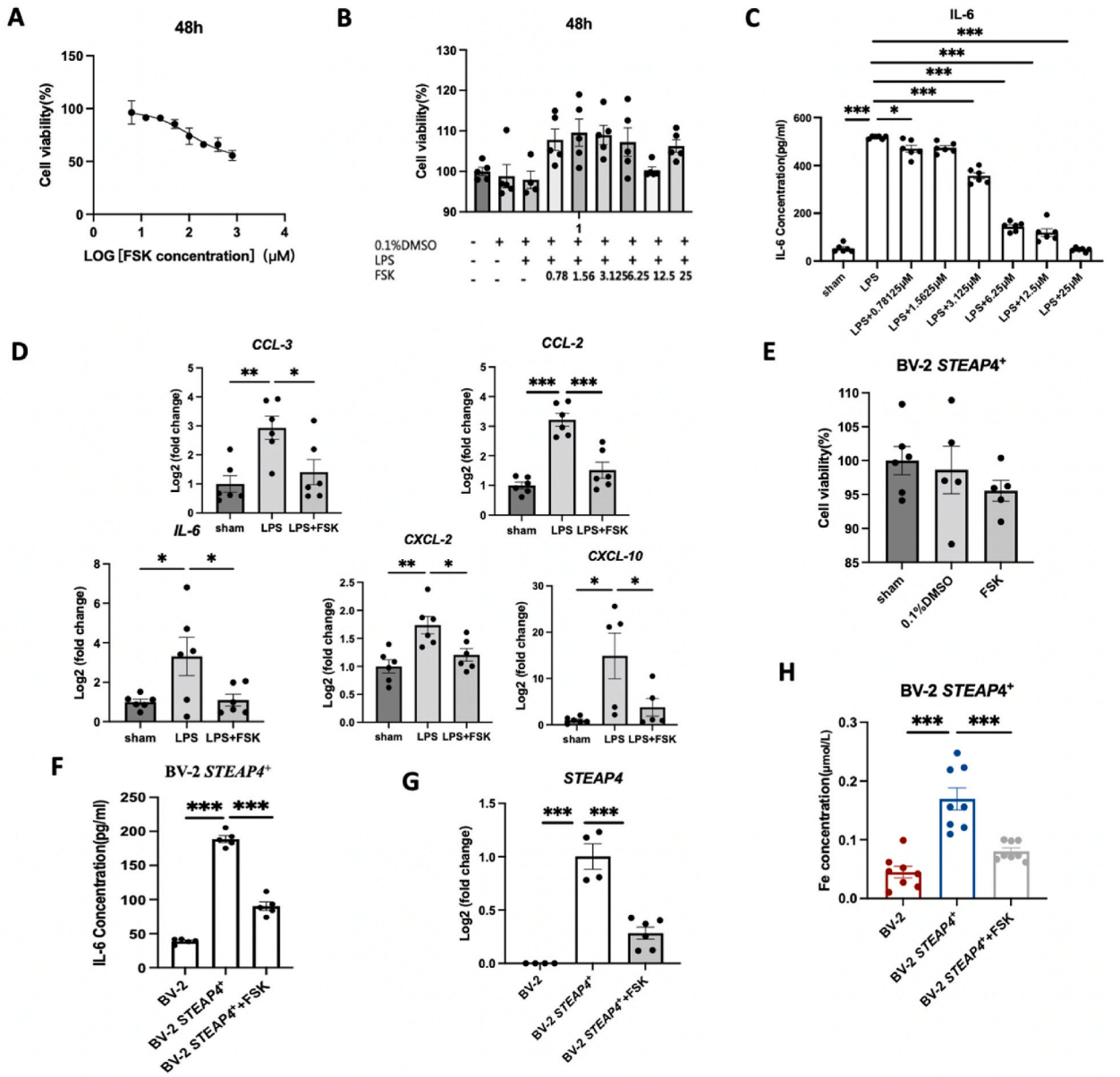

Fig. 3. Effects of FSK on BV-2 cells. (A) Cell viability assay and IC50 calculation, n = 5. (B) The influence of the combination of different concentrations of FSK and LPS on cell viability, n = 5. (C) IL-6 concentration in supernatant was detected by Elisa after 48h of treatment, n = 3. (D) The expressions of CCL-2, CCL-3, IL-6, CXCL-2, and CXCL-10 in BV-2 cells were detected by qPCR after 48 h of treatment, n = 6. (E) CCK-8 assay for cell viability of BV-2 STEAP4^{+} cells, n = 5. (F) The concentration of IL-6 in the supernatant of BV-2 STEAP4^{+} cells was detected by Elisa after 48h of treatment, n = 5. (G) The expression of *STEAP4* in BV-2 STEAP4^{+} cells and normal BV-2 cells was detected by Elisa after 48 h of treatment, and it was further confirmed by qPCR, n = 6. (H) Total iron ion concentration in cell supernatant of BV-2 STEAP4^{+} cells and normal BV-2 cells after 48h treatment of FSK, n = 8 $^{*}P < 0.05$, $^{**}P < 0.01$, $^{***}P < 0.001$.

3.2. FSK stopped the disease process of EAE

From day 1 to day 18, there was little change in body weight in the EAE group, and it showed a loss of appetite, whereas the body weight of sham and FSK mice increased with time, thus FSK administration significantly improved the weight loss in EAE mice (Fig. 4A). In addition, from day 1 to day 18, the clinical scores of the FSK group were significantly lower than those in the EAE group (Fig. 4B). In the open field test, the moving distance and average moving speed of the EAE group were significantly lower than those of the sham group. It was also found that the distance traveled and the average speed of movement in the FSK group were significantly improved compared to the EAE group, and there was no significant difference between the sham group and the FSK group (Fig. 4C). Furthermore, the stained sections of spinal cords in the EAE group significantly showed more unstained areas and light blue areas

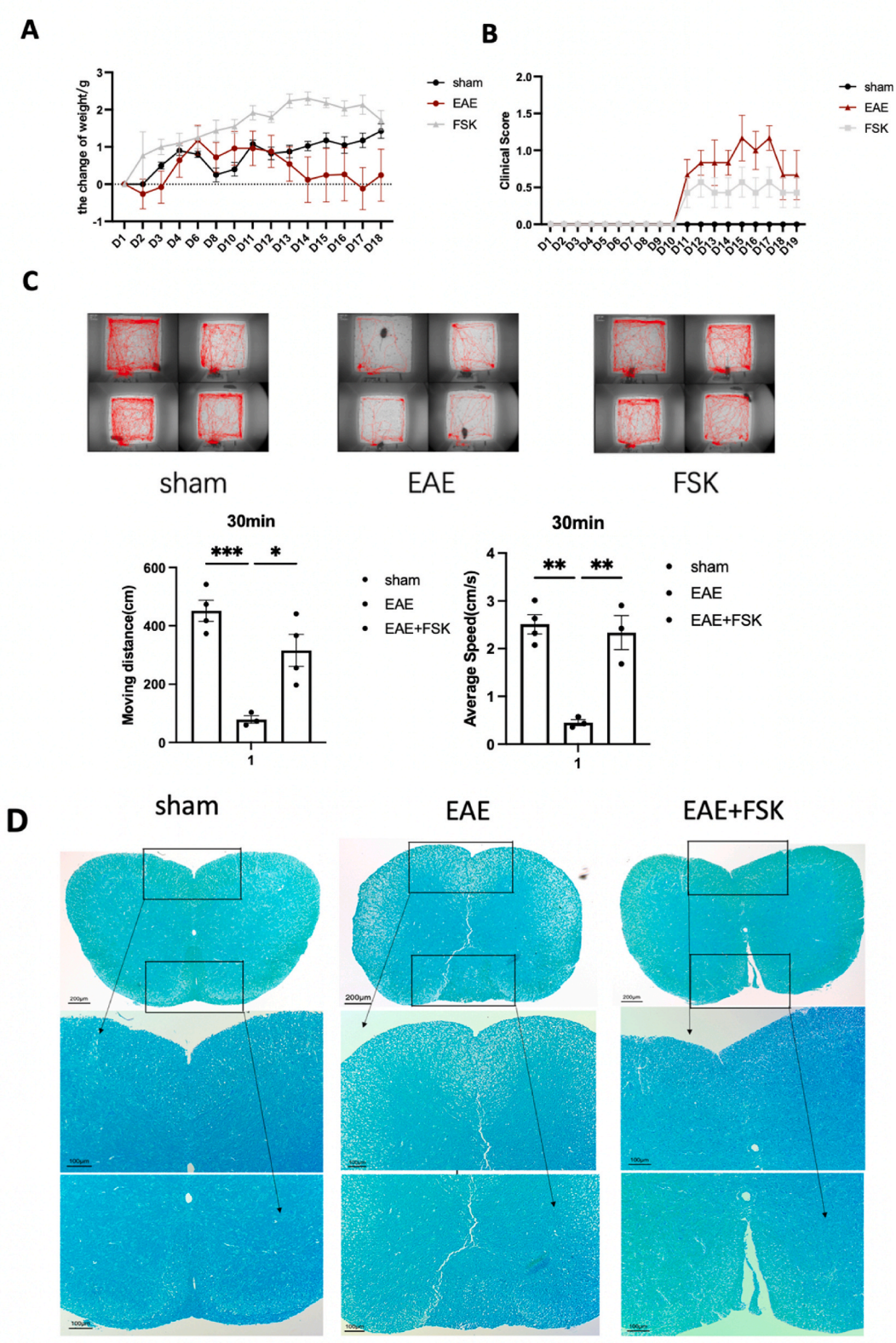

Fig. 4. FSK prevented the onset of EAE. (A) The body weight changes of mice in each group from day 1 to day 18. (B) Clinical scores of mice in each group from day 1 to day 19. (C) The results of the open field test. (D) LFB staining of spinal cords of mice in each group. $^{*}P < 0.05$, $^{**}P < 0.01$, $^{***}P < 0.001$, n = 4~7.

compared to the sham group, which was also improved after FSK treatment (Fig. 4D).

3.3. FSK treatment reduced the number of lymphocytes and the production of pro-inflammatory factors in the spleen and lymph nodes

By calculating the splenic index (SI), it was found that the spleen index in the EAE group was significantly higher than that in the sham group. However, there was a certain degree of decrease in the spleen index in the FSK group compared to the EAE group (Fig. 5B). The results of FC showed that the percentage of $CD4^+$ cells and $CD4^+$ $IL\text{-}17^+$ cells in the lymph nodes and spleen of the EAE group significantly increased compared to the sham group, which was significantly reduced after FSK treatment (Fig. 5A). qPCR results showed that compared with the sham group, the expressions of *IL-17A*, *IL-6*, and *IFN-γ* in spleen tissues of the EAE group significantly increased. After FSK treatment, the expression of *IL-17A* and *IFN-γ* significantly decreased, while the expression of *IL-6* was not statistically altered. In addition, the expressions of *TGF-β* in three groups were not statistically significant (Fig. 5C). In addition, WB results showed that the protein expression of IL-17A was significantly up-regulated in the EAE group compared to the control group; after FSK treatment, its expression decreased significantly (Fig. 5D).

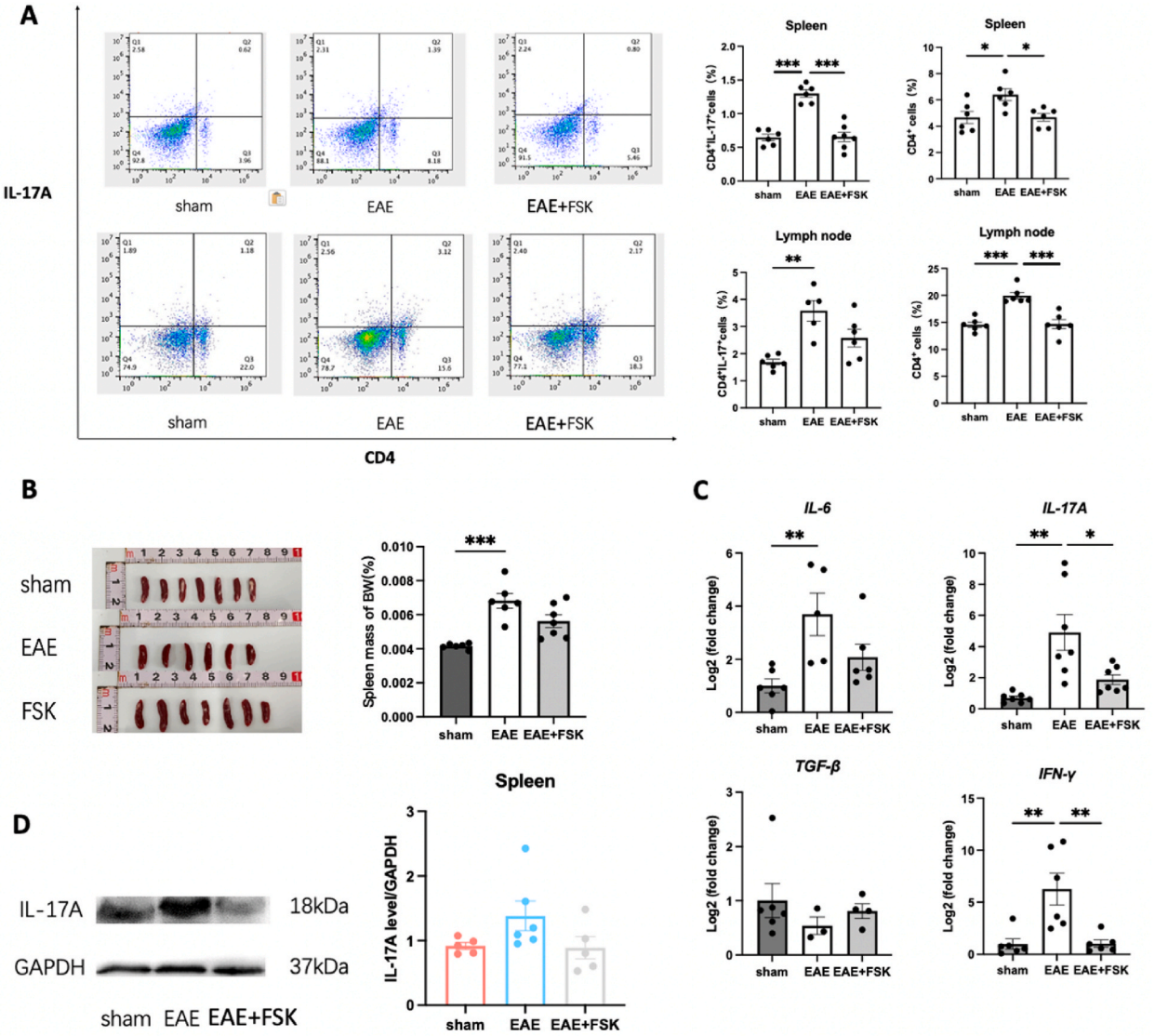

Fig. 5. Effects of FSK treatment on the peripheral immune system. (A) FC assay of the percentage of $CD4^+$ cells and $CD4^+$ $IL\text{-}17^+$ cells in lymph nodes and spleens. (B) Picture of the spleens of mice and spleen index. (C) The mRNA expression levels of *IL-6*, *IL-17A*, *TGF-β*, and *IFN-γ* after 48h treatment with FSK in the spleen. (D) The WB results of IL-17A expression in spleen tissue. $^*P < 0.05$, $^{**}P < 0.01$, $^{***}P < 0.001$, n = 4~7.

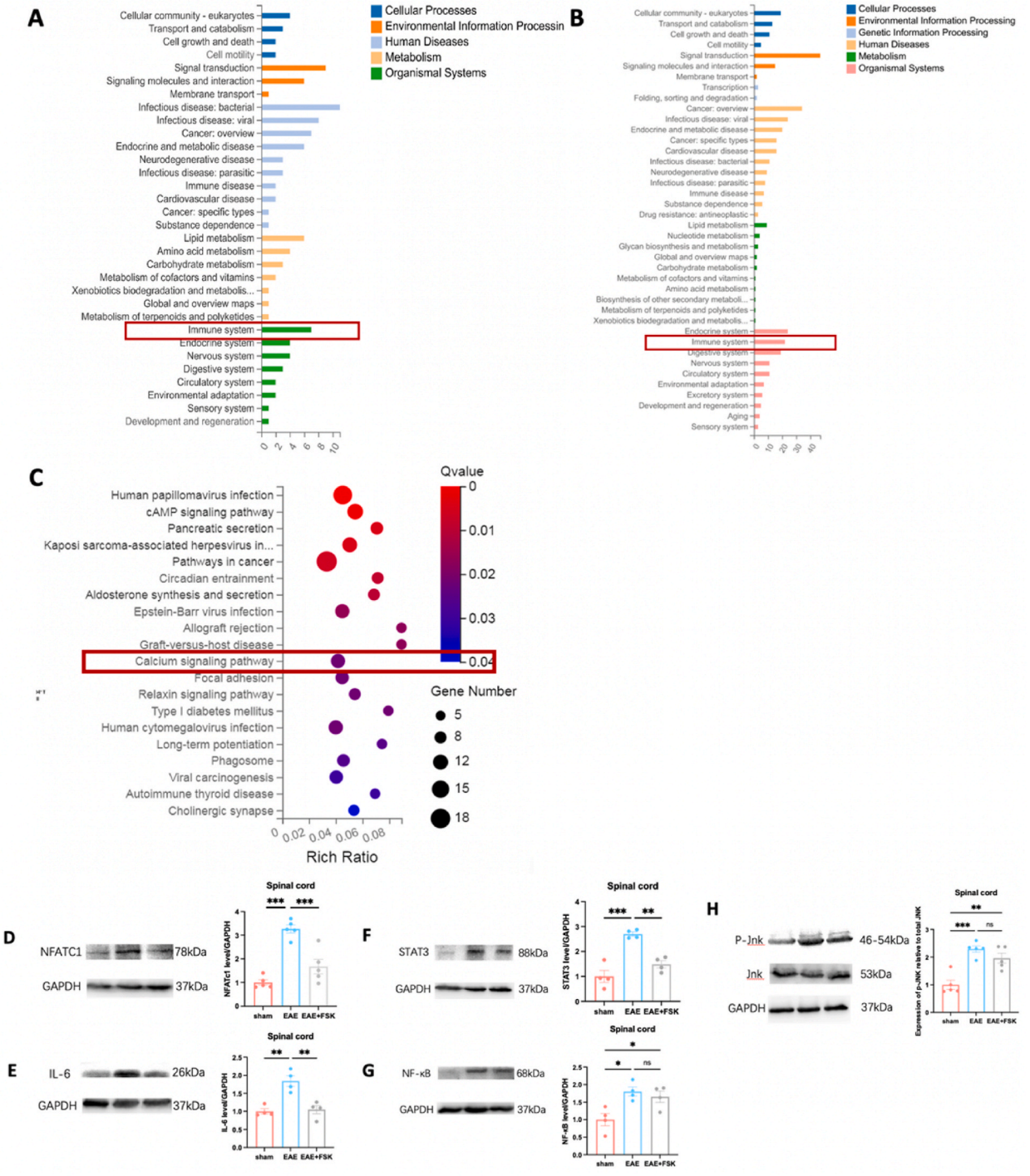

Fig. 6. FSK treatment affected the calcium signaling pathway. (A) Classification map of sham/EAE of differential gene KEGG pathway. (B) Classification map of differential genes by KEGG pathway analysis (FSK treatment group and EAE group). (C) Enrichment map of differential genes by KEGG pathway analysis (FSK treatment group and EAE group). (D) The WB results of NFATc1 expression in the spinal cord. (E) The WB results of IL-6 expression in the spinal cord. (F) The WB results of STAT3 expression in the spinal cord. (G) The WB results of NF-κB expression in the spinal cord. (H) The WB results of expression of p-JNK relative to total JNK in the spinal cord. $^{*}P < 0.05$, $^{**}P < 0.01$, $^{***}P < 0.001$, n = 4∼5.

3.4. FSK treatment affected the calcium signaling pathway

Whole transcriptome sequencing was conducted on the spinal cord to investigate how FSK prevented EAE progression in mice. The differential KEGG pathways in EAE/sham mice were first classified, and it was found that the altered genes were mainly concentrated in the immune system (Fig. 6A). The differential KEGG pathways in EAE/FSK group mice were then classified, and the altered genes were also mainly concentrated in the immune system (Fig. 6B). Therefore, the altered genes in the immune system were focused on the following analysis. Enrichment of differential KEGG pathways in EAE/FSK group mice showed significant changes in the calcium signaling pathway related to TH17 cell differentiation (Fig. 6C).

The calcium signaling pathway-related proteins were verified to investigate whether FSK administration affects TH17 cell differentiation through the calcium signaling pathway. The results showed that the expression of NFATc1 protein associated with the calcium signaling pathway significantly increased in the EAE group compared to the sham group. In contrast, its expression was significantly downregulated after FSK treatment. Besides, there was no significant difference between the sham group and the FSK group (Fig. 6D). In addition, this study also verified the inflammatory pathways related to the calcium signaling pathway. It is reported that LAT protein regulates the calcium signaling pathway, MAPK signaling pathway, and NF-κB signaling pathway [21]. The results showed that the expression levels of NF-κB and p-jnk protein in the EAE group were significantly higher than those in the sham group. However, FSK treatment didn't alter the expression levels of NF-κB and p-jnk. (Fig. 6G and H). Therefore, it is further verified that FSK mainly affects the calcium signaling pathway.

IL-17 is known to stimulate astrocytes to produce inflammatory cytokines such as IL-6 [22]. Therefore, the protein expression levels of IL-6 and STAT3, the positive modulator factors that affect TH17 differentiation, were detected. The results showed that the expression levels of IL-6 and STAT3 protein in the EAE group were significantly increased compared with those in the sham group, which decreased significantly after FSK administration. Besides, there was no significant difference between the sham group and the FSK group (Fig. 6E and F).

3.5. FSK treatment decreased the levels of IL-17A and IFN-γ in peripheral blood

To further investigate the effects of FSK treatment on the cytokines in peripheral blood, the concentrations of IFN-γ and IL-17A in the serum were measured using Elisa assay kits. The results showed that serum concentrations of IFN-γ and IL-17A were significantly increased in the EAE group compared with the sham group, while the levels of both significantly decreased after FSK treatment compared to the EAE group, and there was no significant difference between the FSK treatment group and the sham group (Fig. 7A and B).

3.6. FSK treatment decreased the levels of IL-17A and other pro-inflammatory factors in the spinal cord and brain

To explore the effects of FSK treatment on the levels of IL-17A and other pro-inflammatory factors at the lesion site was detected by western blotting. The results showed that the protein expression of IL-17A significantly increased in the EAE group compared to the sham group, which was remarkably inhibited after FSK treatment. Besides, there was no significant difference between the FSK treatment group and the sham group (Fig. 8A and B). Then, qPCR results showed that the mRNA expression levels of *IL-6*, *IL-17A*, and *IFN-γ* were all significantly increased. In contrast, the expression levels of *TGF-β* remarkably decreased in the EAE group compared to the sham group (Fig. 8C). After FSK treatment, the mRNA expression levels of *IL-6*, *IL-17A*, and *IFN-γ* were all significantly suppressed. while the mRNA expression levels of *TGF-β* were not altered statistically. Meanwhile, this study also detected the mRNA expression levels of chemokines such as *CCL-2* and *CXCL-2*, it was found that the mRNA expression levels of *CCL-2* in the lesion site of the EAE group were significantly elevated compared to the sham group, which were dramatically suppressed after FSK treatment. The mRNA expression level of *CXCL-2* was higher than that of the EAE group, but there was no significant difference (Fig. 8C).

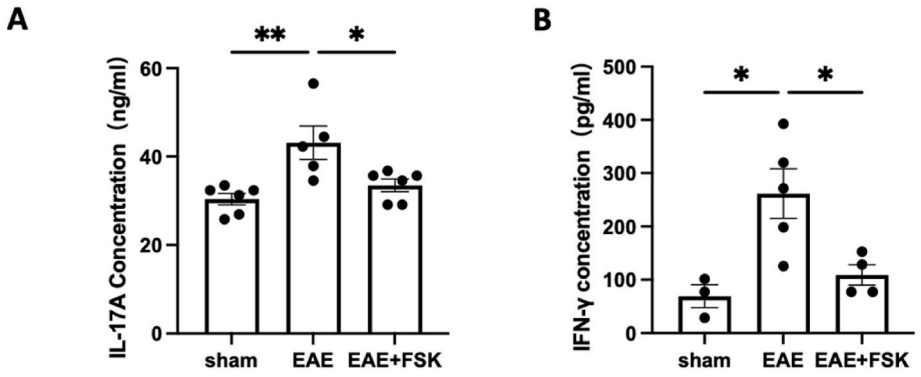

Fig. 7. Effects of FSK treatment on IL-17A and IFN-γ levels in the peripheral blood. (A) The levels of IL-17A in peripheral blood serum. (B) The levels of IFN-γ in peripheral blood serum. $^{*}P < 0.05$, $^{**}P < 0.01$, n = 5~7.

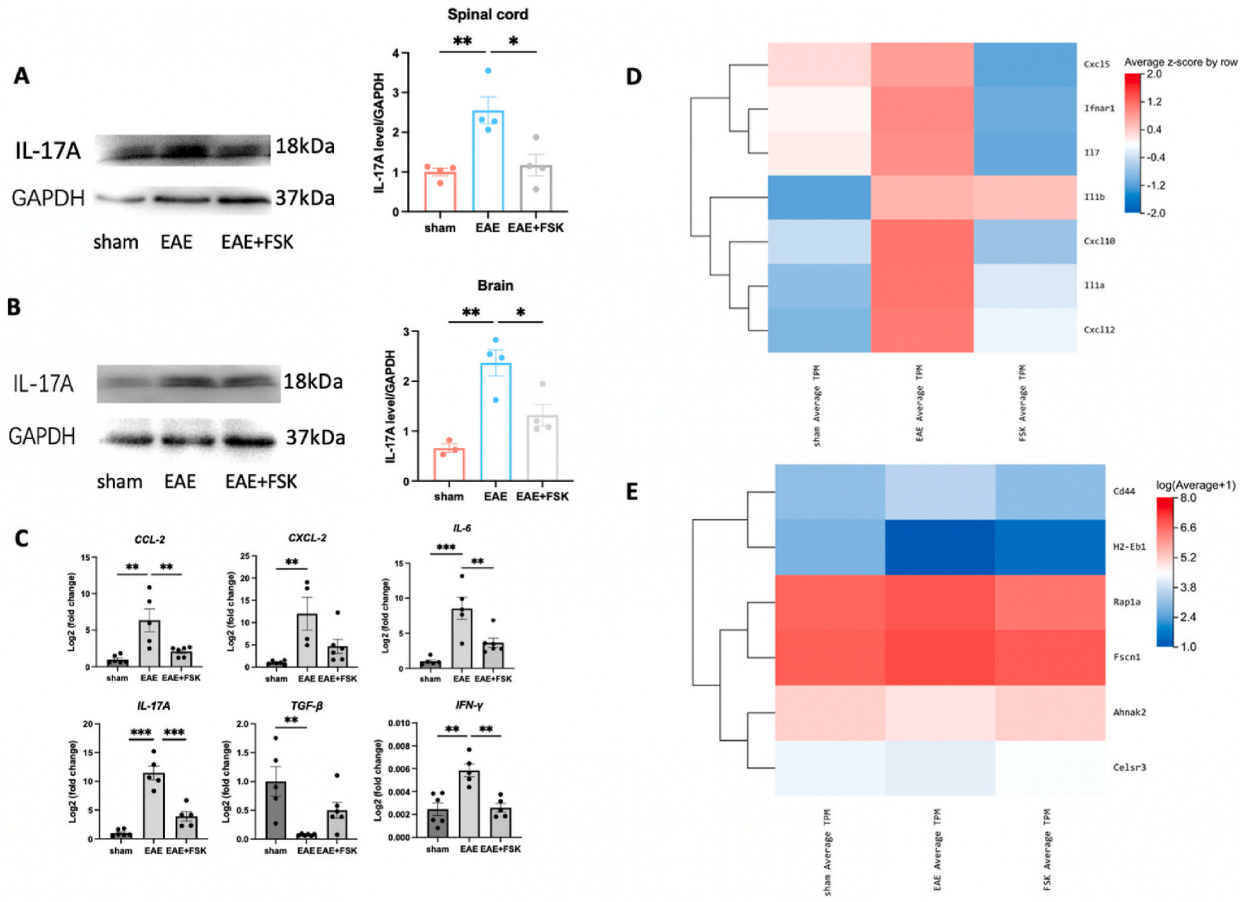

Fig. 8. Effects of FSK treatment on cytokines in brain and spinal cord. (A) The WB results of IL-17A expression in the spinal cord. (B) The WB results of IL-17A expression in the brain. (C) The mRNA expression levels of *IL-6*, *IL-17A*, *TGF-β*, *CCL-2*, *CXCL-2*, and *IFN-γ* after 48h treatment with FSK in the brain were determined by qPCR. (D) Thermogram of differential expression of some pro-inflammatory factors in the spinal cord. (E) Expression cluster heat map of *Cd44*, *H2-Eb1*, *Rap1a*, *FSCN1*, *Ahnak2*, and *Celsr3*. $^{*}P < 0.05$, $^{**}P < 0.01$, $^{***}P < 0.001$, n = 4∼7.

In addition, heat map analysis of proinflammatory factors and chemokines in the spinal cord showed that the expression levels of these pro-inflammatory factors and chemokines in the spinal cord of the EAE group increased compared to the sham group. However, the expression levels of these pro-inflammatory factors and chemokines in the spinal cord decreased after FSK treatment (Fig. 8D). The *Celsr3* gene is involved in the growth and development of nerve axons and dendrites and the formation of nerve fiber networks [23]. As can be seen from the heat map, the expression of the *Celsr3* gene was significantly decreased in the EAE group compared to the sham group, which was remarkably restored after FSK treatment. *H2-Eb1*gene regulates the imbalance of Th1/Th2 and Th17 [24]. Compared with the sham group, *H2-Eb1* gene expression significantly decreased in the EAE group, and the expression level of *H2-Eb1*gene increased significantly after FSK treatment. *Rap1a* gene can participate in and regulate cell growth, differentiation, cytokine synthesis, chemotaxis, and other processes through several important signal transduction pathways [25]. Compared with the sham group, *Rap1a* gene expression was up-regulated in the EAE group. After FSK treatment, *Rap1a* gene expression was downregulated. *Ahnak* gene inhibits the proliferation and invasion of brain glial cells and induces cell apoptosis [26]. Compared with the sham group, *Ahnak* gene expression was up-regulated in the EAE group. After FSK treatment, *Ahnak* gene expression was downregulated. Besides, both *CD44* and *FSCN1* genes were involved in cell interaction, adhesion, and migration [27,28], and their expression level increased in the EAE group compared to the sham group. However, their expression levels decreased after FSK treatment (Fig. 8E).

3.7. FSK treatment decreased the expression of STEAP4 and regulated iron homeostasis

WB results showed that the expression level of STEAP4 in the brain and spinal cord of the EAE group was significantly higher than that of the sham group. In contrast, its expression significantly decreased after FSK treatment (Fig. 9A and B). Meanwhile, qPCR results found that mRNA expression of STEAP4 in the spinal cord and the brain in the EAE group was significantly higher than that in the sham group, which also significantly decreased in the FSK treatment group (Fig. 9C). Previous studies have demonstrated that high STEAP4 expression can cause iron and copper accumulation *in vivo* [14]. After showing that FSK treatment reduces STEAP4 expression, we

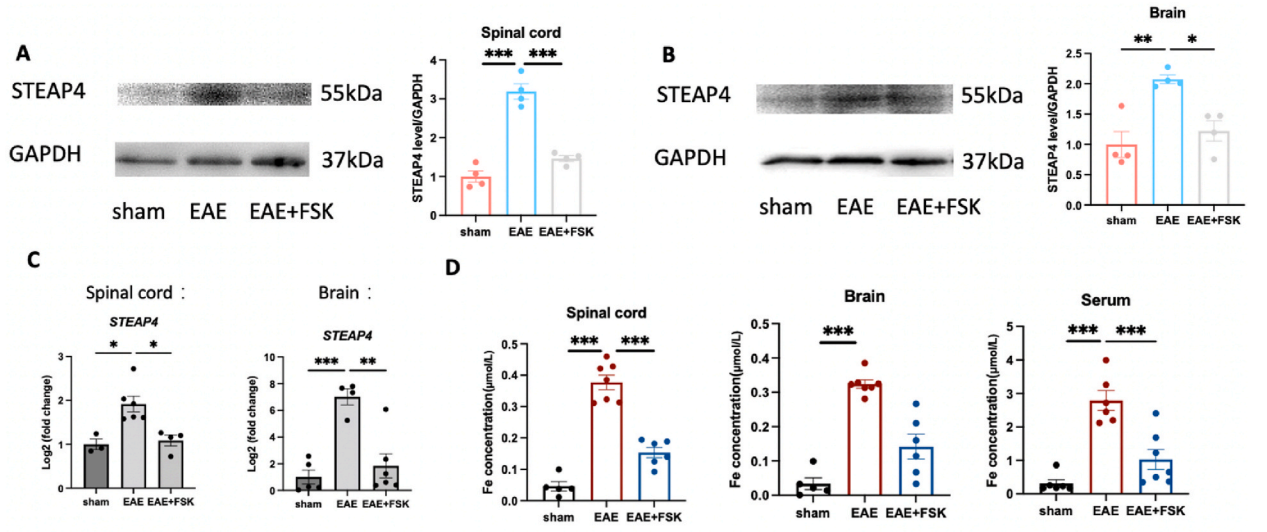

Fig. 9. FSK treatment decreased *STEAP4* expression and regulated iron homeostasis. (A) The WB results of STEAP4 expression in the spinal cord. (B) The WB results of STEAP4 expression in the brain. (C) The mRNA expression of *STEAP4* in the brain and spinal cord after FSK treatment was detected by qPCR. (D) Total iron ion concentration in the brain, spinal cord, and serum after FSK treatment was detected by a total iron ion assay kit. $^{*}P < 0.05$, $^{**}P < 0.01$, $^{***}P < 0.001$, n = 7.

extracted cerebrospinal fluid to determine iron content. We observed a significant increase in total iron concentration in the EAE group compared to the sham group, which was significantly reduced after FSK treatment (Fig. 9D). Additionally, it was also found that the total iron concentration in serum significantly increased in the EAE group compared to the sham group. However, the concentration was remarkably reduced after FSK treatment (Fig. 9D).

4. Discussion

Multiple sclerosis (MS) is a chronic autoimmune condition affecting the CNS. In this condition, the immune system mistakenly identifies myelin sheath as a foreign substance and attacks it. This immune response triggers the release of cytokines and antibodies. Specifically, in the known pathogenesis of MS, $CD4^+$ and $CD8^+$ T cells and B cells are involved in the occurrence and development of the disease. IL-17, mainly secreted by $CD4^+$ cells, can promote the activation of T cells and induce the synthesis and secretion of various cytokines from epithelial cells, endothelial cells, and fibroblasts [9]. IL-17 can also activate microglia to secrete IL-6 and other pro-inflammatory factors and a series of chemokines including CCL-2, CXCL-2, CCL-3, and CXCL-10 [9,29,30]. Therefore, *in vitro* experiments in this study explored whether FSK could inhibit the secretion of IL-6, CCL-2, CCL-3, CXCL-2, and CXCL-10 in BV-2 cells pre-treated by LPS. As an *in vitro* inflammatory stimulator, LPS can induce acute immune response, and stimulate immune cells to produce a large number of pro-inflammatory cytokines, resulting in the overactivation of the immune system [31]. The results in this study showed that compared with the sham group, the levels of IL-6, CCL-2, CCL-3, CXCL-22, and CXCL-10 significantly increased in LPS-treated BV-2 cells. At the same time, FSK treatment suppressed them, suggesting that FSK inhibited the inflammatory response of BV-2 cells induced by LPS. Besides, it was reported that high expression levels of STEAP4 are related to the up-regulation of IL-17, promoting the pathogenesis of EAE [15]. In addition, IL-17 can promote the increase of intracellular Fe levels and induce the high expression of STEAP4, which maintains the activity of NF-κB [32]. Furthermore, the enhanced Caspase-3 activity induced by XIAP, and the apoptotic process induced by inflammation are promoted, leading to extensive neuronal inflammatory damage [33,34]. Therefore, we suspect that there may be interactive regulation of IL-17- STEAP4 to balance inflammatory response and iron homeostasis. To explore how FSK can affect the expression level of IL-6 and iron balance in BV-2 cells, this study investigated whether FSK can alter the expression of STEAP4. Due to the initial low expression of STEAP4 in BV-2 cells, it was undetectable through qPCR. Cells were engineered to overexpress STEAP4 to tackle this problem. The results indicated that after FSK treatment, the content of IL-6 and the expression of STAEP4 in BV-2 STEAP4 overexpression cells were reduced, and the iron homeostasis was maintained, suggesting that FSK treatment can effectively relieve LPS-induced cell inflammatory response possibly by inhibiting the expression of STEAP4 and reducing the iron deposition.

The animal experiment was conducted based on the results of the *in vitro* experiment. The clinical score of EAE mice was significantly higher than that of the sham group, suggesting that the modeling of EAE was successful. However, the clinical scores of EAE mice decreased after FSK administration. Meantime, their activity level, movement speed, and demyelination were improved, indicating that FSK treatment can improve the disease course of EAE. More interestingly, it was found that mice treated with FSK began to lose weight on the 17th day compared to other groups; we speculated that it might be an off-target effect caused by the weight-loss function of FSK [17].

Pro-inflammatory factors and chemokines can induce directed chemotaxis movement of nearby immune cells to the site of infection

during the immune response. Studies have found that up-regulation of pro-inflammatory factors and chemokines can aggravate the onset of EAE and enhance the proliferation and migration of T cells [35,36]. In this study, serum levels of IFN-γ and IL-17A in the EAE group were significantly higher than that in the sham group. However, they dramatically decreased after FSK treatment, indicating that FSK inhibited the production of inflammatory factors in peripheral blood.

The spleen index in the EAE group was significantly higher than that in the sham group. However, it significantly decreased after FSK treatment, suggesting that FSK treatment alleviated the increase in spleen index. FSK treatment also reduced the number of $CD4^+$ cells, and pro-inflammatory factors including IL-6, IL-17A, IFN-γ, as well as chemokines including CCL-2, CXCL-2, CCL-3, and CXCL-10. These findings were similar to a report by Sullivan [37], which found that the CNS inflammation in MOG-EAE models can be improved by inhibiting immune cell activation, cytokine production, and the development of Th17 cells. Thus, we speculated that FSK may inhibit CNS inflammation by correcting immune imbalance.

Transcriptome gene sequencing was performed on the mouse spinal cord to further reveal related mechanisms. The differential genes in the EAE/sham group were mainly concentrated in the immune system. Analysis of the KEGG enrichment pathway in the EAE/FSK group showed significant alterations in the calcium signaling pathway related to TH17 cell differentiation. WB results confirmed that the expression of NFATc1, a core protein member of the calcium signaling pathway, significantly decreased, indicating that FSK inhibited the calcium signaling pathway. However, the MAPK and NF-κB signaling pathway-related proteins did not change significantly, confirming that FSK treatment affected the calcium signaling pathway rather than the NF-κB involved classic inflammatory pathways. Furthermore, multiple studies have reported that IL-17 can activate microglia to secrete IL-6, and both IL-6 and STAT3 are important positive modulators in the TH17 cell differentiation pathway [22,38]. Thus, IL-6 and STAT3 protein levels were determined by WB, and it was found that they decreased significantly after FSK administration. Therefore, we speculate that FSK may improve EAE by inhibiting the calcium signaling pathway, decreasing IL-6 secretion, and regulating TH17 cell differentiation.

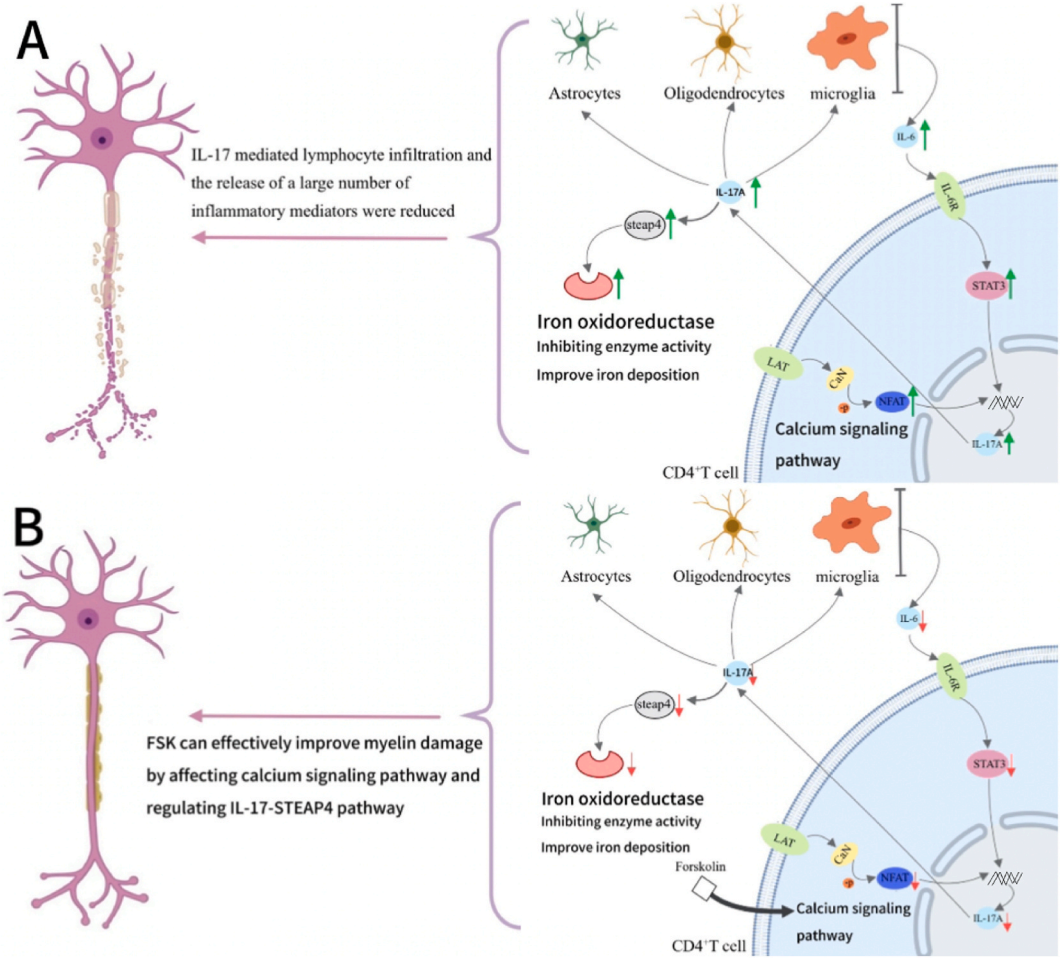

Fig. 10. The possible mechanism by which FSK improves the disease course of EAE mice. (A) The immune system attacks myelin as a foreign substance to enhance inflammatory infiltration, increase the expression of STEAP4, and increase the deposition of iron ions in EAE. (B) FSK reduces IL-17A secretion and STEAP4 expression probably by inhibiting the calcium signaling pathway to balance the iron environment and improve inflammatory infiltration in EAE.

This study also found that the levels of pro-inflammatory factors such as IL-17 and chemokines such as CCL-2 in the spinal cord and brain lesions were significantly increased in EAE mice. However, after FSK treatment, the levels of proinflammatory factors and chemokines in the spinal cord and brain lesions were significantly reduced in EAE mice. Differentially expressed genes from spinal cord transcriptome sequencing data were mainly focused on the immune system, including *Cd44*, *H2-Eb1*, *Rap1a*, *Fscn1*, *Ahnak2*, and *Celsr3*. Analyzing these differential genes suggested that FSK treatment may improve the pathogenesis of EAE mice by regulating Th1/Th2 and Th17 imbalances, inhibiting immune cell proliferation and migration, and reducing cytokine production. In addition, the expression of chemokines and cytokines decreased in the CNS of FSK mice, proving that the inflammatory process was suppressed after FSK administration.

Furthermore, the metal reductase STEAP4 is a key effector molecule that participates in and promotes the pathogenesis of TH17-mediated neuroinflammation in EAE mice, and the occurrence of EAE can induce high expression of STEAP4 in turn [15,39]. This study found that the expression of STEAP4 was significantly decreased in the spinal cord and brain, and the total iron content in the spinal cord and brain tissue also decreased after FSK treatment, suggesting that FSK may regulate inflammatory response and iron homeostasis and improve the symptoms of EAE by reducing IL-17 production and STEAP4 expression.

Combined with the above results, we speculate that FSK treatment may reduce IL-17 secretion, inhibit $CD4^+$ cell proliferation, and reduce cytokine production by inhibiting the calcium signaling pathway and regulating the IL-17-STEAP4 pathway, as shown in Fig. 10. However, the detailed mechanism remains uncovered, and further investigation is required to explore FSK's potential protective pharmacological effects on glial cells and neurons.

5. Conclusion

In conclusion, we have confirmed the ameliorative effect of FSK on EAE at both the cellular and animal levels. This effect may be associated with the inhibition of the calcium pathway and the IL-17-STEAP4 pathway. Our results suggest that FSK may hold the potential for future clinical use in treating MS, and more research is needed to determine the safety and effectiveness of using FSK to treat MS.

Credit statement

All authors hereby declare that we are committed to the authenticity and accuracy of all data in this paper, as well as the standardization of animal experiments. We accept responsibility and consequences for any academic misconduct.

Data availability statements

The data that support the findings of this study are openly available.

CRediT authorship contribution statement

Qinyao Yu: Writing – original draft. **Mengqing Li:** Software. **Umer Anayyat:** Methodology. **Cai Zhou:** Methodology. **Shenglan Nie:** Methodology. **Hua Yang:** Methodology. **Fengyi Chen:** Methodology. **Shuling Xu:** Methodology. **Yunpeng Wei:** Writing – review & editing, Supervision. **Xiaomei Wang:** Writing – review & editing, Supervision.

Declaration of competing interest

The authors declare that they have no known competing financial interests or personal relationships that could have appeared to influence the work reported in this paper.

Acknowledgments

This project was funded by the National Natural Science Foundation of China (NSFC) (No. 81772002), the Shenzhen Science Technology and Innovation Commission (No. JCYJ20230808104859039, No. JCYJ20170818143334365).

Appendix A. Supplementary data

Supplementary data to this article can be found online at https://doi.org/10.1016/j.heliyon.2024.e36063.

References

[1] H. Abboud, E. Hill, J. Siddiqui, A. Serra, B. Walter, Neuromodulation in multiple sclerosis, Mult. Scler. J 23 (13) (2017) 1663–1676.
[2] M. Sarmadi, Z. Bidel, F. Najafi, R. Ramakrishnan, F. Teymoori, H.A. Zarmehri, M. Nazarzadeh, Copper concentration in multiple sclerosis: a systematic review and meta-analysis, Mult Scler Relat Dis 45 (2020).

[3] M.S. Bassi, F. Mori, F. Buttari, G.A. Marfia, A. Sancesario, D. Centonze, E. Iezzi, Neurophysiology of synaptic functioning in multiple sclerosis, Clin. Neurophysiol. 128 (7) (2017) 1148–1157.
[4] A. Busnelli, A. Navarra, P.E. Levi-Setti, Qualitative and quantitative ovarian and peripheral blood mitochondrial DNA (mtDNA) alterations: mechanisms and implications for female fertility, Antioxidants-Basel 10 (1) (2021).
[5] L. Leocani, R. Chieffo, A. Gentile, D. Centonze, Beyond rehabilitation in MS: insights from non-invasive brain stimulation, Mult. Scler. J 25 (10) (2019) 1363–1371.
[6] D.P. Wolf, N. Mitalipov, S. Mitalipov, Mitochondrial replacement therapy in reproductive medicine, Trends Mol. Med. 21 (2) (2015) 68–76.
[7] Z.M. Zhang, Z.Y. Xue, Y. Liu, H.K. Liu, X.D. Guo, Y. Li, H.W. Yang, L.J. Zhang, Y.R. Da, Z. Yao, R.X. Zhang, MicroRNA-181c promotes Th17 cell differentiation and mediates experimental autoimmune encephalomyelitis, Brain Behav. Immun. 70 (2018) 305–314.
[8] N. Dargahi, M. Katsara, T. Tselios, M.E. Androutsou, M. de Courten, J. Matsoukas, V. Apostolopoulos, Multiple sclerosis: immunopathology and treatment update, Brain Sci. 7 (7) (2017).
[9] A. Waisman, J. Hauptmann, T. Regen, The role of IL-17 in CNS diseases, Acta Neuropathol. 129 (5) (2015) 625–637.
[10] S. Farouk, S. Sabet, F.A. Abu Zahra, A.A. El-Ghor, Bone marrow derived-mesenchymal stem cells downregulate IL17A dependent IL6/STAT3 signaling pathway in CCl4-induced rat liver fibrosis, PLoS One 13 (10) (2018).
[11] B.F. Popescu, J.M. Frischer, S.M. Webb, M. Tham, R.C. Adiele, C.A. Robinson, P.D. Fitz-Gibbon, S.D. Weigand, I. Metz, S. Nehzati, G.N. George, I.J. Pickering, W. Bruck, S. Hametner, H. Lassmann, J.E. Parisi, G. Yong, C.F. Lucchinetti, Pathogenic implications of distinct patterns of iron and zinc in chronic MS lesions, Acta Neuropathol. 134 (1) (2017) 45–64.
[12] J. Haas, K. Schneider, A. Schwarz, M. Korporal-Kuhnke, S. Faller, F. von Glehn, S. Jarius, B. Wildemann, Th17 cells: a prognostic marker for MS rebound after natalizumab cessation? Mult. Scler. J 23 (1) (2017) 114–118.
[13] A. Beringer, M. Noack, P. Miossec, IL-17 in chronic inflammation: from discovery to targeting, Trends Mol. Med. 22 (3) (2016) 230–241.
[14] L. De Riccardis, A. Buccolieri, M. Muci, E. Pitotti, F. De Robertis, G. Trianni, D. Manno, M. Maffia, Copper and ceruloplasmin dyshomeostasis in serum and cerebrospinal fluid of multiple sclerosis subjects, Bba-Mol Basis Dis 1864 (5) (2018) 1828–1838.
[15] J.J. Zhao, Y. Liao, W. Miller-Little, J.X. Xiao, C.N. Liu, X.X. Li, X. Li, Z.Z. Kang, STEAP4 expression in CNS resident cells promotes Th17 cell-induced autoimmune encephalomyelitis, J. Neuroinflammation 18 (1) (2021).
[16] B.A. Yu, J.J. Liu, J. Cheng, L. Zhang, C. Song, X.F. Tian, Y.X. Fan, Y. Lv, X. Zhang, A static magnetic field improves iron metabolism and prevents high-fat-diet/streptozocin-induced diabetes, Innovation-Amsterdam 2 (1) (2021).
[17] R.H. Alasbahi, M.F. Melzig, Plectranthus barbatus: a review of phytochemistry, ethnobotanical uses and pharmacology - Part 2, Planta Med. 76 (8) (2010) 753–765.
[18] P. Kapewangolo, A.A. Hussein, D. Meyer, Inhibition of HIV-1 enzymes, antioxidant and anti-inflammatory activities of Plectranthus barbatus, J. Ethnopharmacol. 149 (1) (2013) 184–190.
[19] H. Zhao, A.H. Liu, L.Q. Shen, C.P. Xu, Z.W. Zhu, J.R. Yang, X.L. Han, F.K. Bao, W.M. Yang, Isoforskolin downregulates proinflammatory responses induced by Borrelia burgdorferi basic membrane protein A, Exp. Ther. Med. 14 (6) (2017) 5974–5980.
[20] W.M. Yang, D.J. Qiang, M. Zhang, L.M. Ma, Y.H. Zhang, C. Qing, Y.L. Xu, C.L. Zhen, J.K. Liu, Y.H. Chen, Isoforskolin pretreatment attenuates lipopolysaccharide-induced acute lung injury in animal models, Int. Immunopharm. 11 (6) (2011) 683–692.
[21] M. Martinez-Florensa, A. Garcia-Blesa, J. Yelamos, A. Munoz-Suano, M. Dominguez-Villar, R. Valdor, A. Alonso, F. Garcia-Cozar, P. Aparicio, B. Malissen, E. Aguado, Serine residues in the LAT adaptor are essential for TCR-dependent signal transduction, J. Leukoc. Biol. 89 (1) (2011) 63–73.
[22] J.J. Graber, S.R. Allie, K.M. Mullen, M.V. Jones, T.G. Wang, C. Krishnan, A.I. Kaplin, A. Nath, D.A. Kerr, P.A. Calabresi, Interleukin-17 in transverse myelitis and multiple sclerosis, J. Neuroimmunol. 196 (1–2) (2008) 124–132.
[23] Q.J. Zhou, J.W. Qin, Y.Y. Liang, W. Zhang, S.Y. He, F. Tissir, Y.B. Qu, L.B. Zhou, Celsr3 is required for Purkinje cell maturation and regulates cerebellar postsynaptic plasticity, iScience 24 (7) (2021).
[24] L.G. Li, B. Hu, J. Feng, Y. Zhang, X. Shou, Y. Tian, C.R. Jiang, H. Zhang, H2-EB1 molecule alleviates allergic rhinitis symptoms of H2-eb1 knockout mice, Iran J Immunol 12 (4) (2015) 263–273.
[25] V. Pizon, G. Baldacci, Rap1A protein interferes with various MAP kinase activating pathways in skeletal myogenic cells, Oncogene 19 (52) (2000) 6074–6081.
[26] S. Shin, J.K. Seong, Y.S. Bae, Ahnak stimulates BMP2-mediated adipocyte differentiation through Smad1 activation, Obesity 24 (2) (2016) 398–407.
[27] L. Li, L.H. Chen, Z.W. Li, S.Q. Huang, Y.Y. Chen, Z.Y. Li, W.K. Chen, FSCN1 promotes proliferation, invasion and glycolysis via the IRF4/AKT signaling pathway in oral squamous cell carcinoma, BMC Oral Health 23 (1) (2023).
[28] A.J. Ruiz-Moreno, A. Reyes-Romero, A. Domling, M.A. Velasco-Velazquez, In silico design and selection of new tetrahydroisoquinoline-based CD44 antagonist candidates, Molecules 26 (7) (2021).
[29] J. Hong, H.Y. Li, M.Y. Chen, Y.C.Q. Zang, S.M. Skinner, J.M. Killian, J.Z.W. Zhang, Regulatory and pro-inflammatory phenotypes of myelin basic protein-autoreactive T cells in multiple sclerosis, Int. Immunol. 21 (12) (2009) 1329–1340.
[30] D.J. Mahad, R.M. Ransohoff, The role of MCP-1 (CCL2) and CCR2 in multiple sclerosis and experimental autoimmune encephalomyelitis (EAE), Semin. Immunol. 15 (1) (2003) 23–32.
[31] T.K. Park, S. Koppula, M.S. Kim, S.H. Jung, H. Kang, Anti-neuroinflammatory effects of houttuynia cordata extract on LPS-stimulated BV-2 microglia, Trop. J. Pharmaceut. Res. 12 (4) (2013) 523–528.
[32] R. Dubbioso, L. Ruggiero, M. Esposito, P. Tarantino, M. De Angelis, F. Aruta, S. Pappatà, L. Ugga, A. Piperno, R. Iorio, L. Santoro, R. Iodice, F. Manganelli, Different cortical excitability profiles in hereditary brain iron and copper accumulation, Neurol. Sci. 41 (3) (2020) 679–685.
[33] M. Irony-Tur-Sinai, M. Lichtenstein, T. Brenner, H. Lorberboum-Galski, IL2-caspase3 chimeric protein controls lymphocyte reactivity by targeted apoptosis, leading to amelioration of experimental autoimmune encephalomyelitis, Int. Immunopharm. 9 (10) (2009) 1236–1243.
[34] C.S. Moore, A.L.O. Hebb, M.M. Blanchard, C.E. Crocker, P. Liston, R.G. Korneluk, G.S. Robertson, Increased X-linked inhibitor of apoptosis protein (XIAP) expression exacerbates experimental autoimmune encephalomyelitis (EAE), J. Neuroimmunol. 203 (1) (2008) 79–93.
[35] C. Weissleder, M.J. Webster, C.S. Weickert, Reduced chemokine signalling capacity is associated with inhibitory interneuron dysfunction in subcortical brain regions in schizophrenia and bipolar disorder, Schizophr. Bull. 46 (2020) S202–S203.
[36] T.Y. Zhan, X.M. Wang, Z.J. Ouyang, Y.L. Yao, J.Y. Xu, S.K. Liu, K. Liu, Q.Y. Deng, Y.S. Wang, Y.Y. Zhao, Rotating magnetic field ameliorates experimental autoimmune encephalomveigis by promoting T cell peripheral accumulation and regulating the oalance of Treg and Th1/Th17, Aging-Us 12 (7) (2020) 6225–6239.
[37] J. Sullivan, C. Brown, M. Mayo, V. Dixit, B. Enerson, H. Rong, B. Yang, C. De Savi, J. Gollob, N. Mainolfi, A. Slavin, C. Hubeau, STAT3 degraders inhibit cellular activation, cytokine production, and Th17 development, resulting in inhibition of autoimmunity in the MOG-EAE model of CNS inflammation, J. Immunol. 208 (1) (2022).
[38] M. Nyirenda, C. Constantinescu, G. Podda, A. Bar-Or, G.X. Zhang, B. Gran, Toll-like receptor 2 (TLR2) stimulation regulates the balance between Th17 and Treg function in multiple sclerosis: a key role for IL-6/STAT3 signalling, J. Neuroimmunol. 253 (1–2) (2012), 109-109.
[39] V. Catalán, J. Gómez-Ambrosi, A. Rodríguez, B. Ramírez, F. Rotellar, V. Valentí, C. Silva, M.J. Gil, J. Salvador, G. Frühbeck, Six-transmembrane epithelial antigen of prostate 4 and neutrophil gelatinase-associated lipocalin expression in visceral adipose tissue is related to iron status and inflammation in human obesity, Eur. J. Nutr. 52 (6) (2013) 1587–1595.